JOURNAL OF MATERIALS SCIENCE **33** (1998) 5677–5682

A fine cobalt-toughened Al_2O_3-TiC ceramic and its wear resistance

D. S. MAO, X. H. LIU
Ion Beam Laboratory, Shanghai Institute of Metallurgy, Chinese Academy of Sciences, Shanghai 200050, People's Republic of China
E-mail: xhliu@fudan.ihep.ac.cn

J. LI, S. Y. GUO, X. B. ZHANG, Z. Y. MAO
Department of Materials Science and Engineering, Zhejiang University, Hangzhou 310027, People's Republic of China

Mechanical ball milling is the most common method for mixing ceramic powders with a ductile phase such as metal particles. In this paper, a new powder processing way is presented. Al_2O_3 and TiC powders are coated with a layer of metal cobalt using the chemical deposition process. The thickness of the metal cobalt film can be controlled by adjusting the deposition conditions. The Co-coated Al_2O_3 (Al_2O_3–Co) and TiC (Tic–Co) powders are mixed at the rate of 7 : 3 and hot-press sintered into a fine Al_2O_3–TiC–Co (ATC) ceramic. The main properties, erosion behaviour, abrasion behaviour, wear mechanism and wear resistance of Al_2O_3-TiC-Co and Al_2O_3–30 wt % TiC (AT_{30}) ceramics are determined by transmission electron microscopy, scanning electron microscopy, energy dispersive X-ray spectroscopy, etc. It is shown that the ATC ceramic possesses improved mechanical properties. Because of the existence of metal cobalt in the grain boundaries, the bonding strength between grains is increased, and this prevents spalling of grains during wear. Experimentation indicates that ATC is more resistant to wear than Al_2O_3–TiC ceramic. The relationship between their mechanical properties and wear resistance is also discussed in this paper.

1. Introduction

Al_2O_3–TiC ceramics have been widely used as cutting tools this decade because of their chemical stability, high strength and hardness, etc., especially excellent wear resistance [1–3]. In this kind of ceramic, TiC shows relatively higher hardness and melting point, and the refining effect of TiC dispersed in the matrix after sintering is remarkable. TiC can prevent crack propagation [4], and therefore improve the mechanical properties of Al_2O_3-based ceramics, especially the fracture toughness and hardness. It is generally accepted that when the content of TiC is about 30 wt % in the Al_2O_3 matrix, the ceramic (namely AT_{30}) possesses most excellent properties [5]. But there are still some defects in this kind of ceramic, such as pores in the matrix, reactions between Al_2O_3 and TiC at high temperatures during sintering [1], etc., which cannot be overlooked. These defects obviously decrease the mechanical properties and wear resistance of the ceramic. If these problems can be limited/prevented, then perfect Al_2O_3–TiC ceramics can be obtained.

It has been pointed out that fracture toughness and hardness are the most important mechanical properties in the wear of brittle materials such as Al_2O_3-based ceramics [6–8]. For common ceramics, it is noted that improving fracture toughness to a fit value can improve wear resistance [9]. Up to now, a series of strengthening mechanisms have been proposed, including a phase transformation toughening mechanism, such as zirconia-toughened ceramics, a second particle enforcement mechanism, a fine grain strengthening mechanism, and fibre or whisker reinforcing technology, etc. [10]. In this paper, a newly developed powder metallurgy technology is presented. A thin layer of metal cobalt is coated onto Al_2O_3 and TiC powders. Compared with AT_{30} ceramic, the hot-pressed Al_2O_3–TiC–Co (ATC) ceramic possesses improved mechanical properties. Its fracture toughness and bending strength increase about 40%. It is more resistant to wear than AT_{30} ceramic.

2. Experimental procedure

Al_2O_3 and TiC powders are coated with metal cobalt films by chemical deposition to obtain Al_2O_3–Co and TiC–Co composite powders. The two kind of powders are mixed in the ratio 7 : 3, then hot-pressed into ATC ceramic. A mixture of Al_2O_3 and 30 wt % TiC powders is hot-pressed into AT_{30} ceramic.

The bending strength of the samples is measured by a three-point bending test, with a span of 30 mm and a loading speed of 0.5 mm min^{-1} (the size of the samples is $3 \times 4 \times 34$ mm). Vickers hardness and fracture toughness are evaluated by the microindentation

TABLE I Composition and properties of the test ceramics

Materials	Composition (wt %)			Density (g cm^{-3})	Vickers hardness, H_V	Fracture toughness (MPa m$^{-1/2}$)	Bending strength (GPa)
	Al_2O_3	TiC	Co				
AT_{30}	71.4	28.6	0	4.16	2073	5.2	536
ATC	67.0	27.9	5.1	4.35	1954	7.9	714

technique, with a Vickers diamond indenter at loads between 50 and 300 N. The density of the samples is tested by liquid weighing. The microstructure of the samples is analysed by transmission electron microscopy (TEM). The chemical composition of the test samples is detected by energy dispersive X-ray spectroscopy (EDXS) (Table I).

The air-borne particle test is used to analyse erosion wear resistance of the ceramics. Impingement velocities are 30, 65 and 90 m s^{-1}. Impact angles are arranged to 15, 30, 45, 60, 75 and 90°. The dry sand rubber wheel test is employed to analyse the abrasion wear resistance of the ceramics: the test is performed at loads of 40, 100 and 228 N. Angular SiC particles (120–150 μm) are used in both tests, in addition SiO_2 particles (120–150 μm) are also used in the abrasion wear test. Before the tests, ATC and AT_{30} ceramics are polished with diamond paste. A balance with a sensitivity of 10^{-5} g is used to analyse the mass loss in wear. The experiment was repeated three times for each condition and the average values plotted. The worn surfaces are observed by scanning electron microscopy (SEM), with special attention to grain detachment, crack development and plastic deformation.

3. Results

3.1. Erosion

Fig. 1 shows the erosion rate of the samples versus impingement angles caused by an SiC particle impacting at 90 m s^{-1} blasting velocity. The erosion rate of the ceramics increases with increasing impact angle, and the maximum erosion rate value appears at an angle of nearly 90°. Approximately, the erosion rate of the ATC ceramic drops by 30% compared with the AT_{30} ceramic.

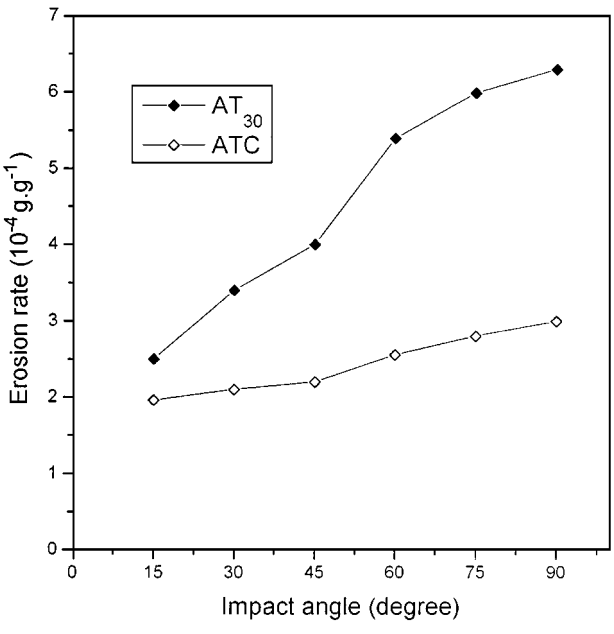

Figure 1 Erosion rate of the samples versus different impingement angles of SiC particles at 90 m s^{-1} blasting velocity.

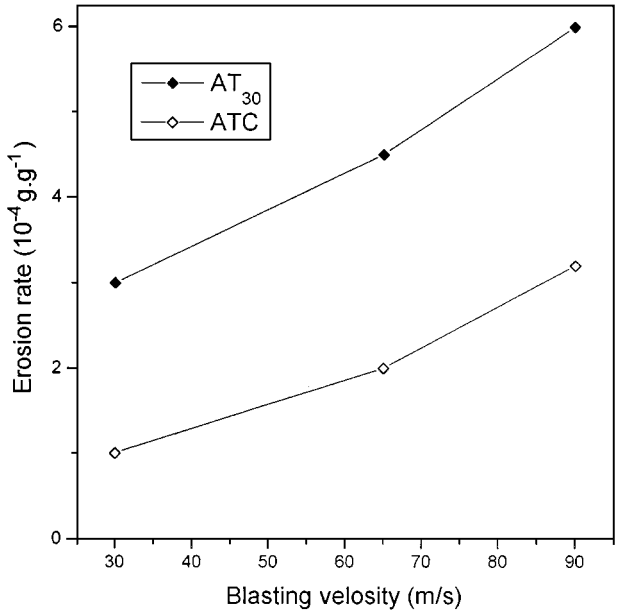

Figure 2 Erosion rate of the samples at different blasting velocities at a 90° impact angle.

Fig. 2 illustrates the wear behaviour of samples at different blasting velocities, which demonstrates that the wear rate of the two types of samples increases with increasing blasting velocity, implying that increasing particle velocity at constant particle size, i.e. increasing the instantaneous surface impact stress, can cause increased deformation and fracture. A critical amount of deformation will give rise to the initiation of microcracks and result in material removal following further propagation of these cracks.

Fig. 3a is an SEM image of the eroded surface of AT_{30} ceramic at 90 m s^{-1} blasting velocity at an impact angle of 90°, showing lateral cracking and deep detaching. Fig. 3b is an SEM image of eroded ATC ceramic at 90 m s^{-1} blasting velocity at an impact angle of 90°. It is shown that there are microcracks, shallow detachments and plastic deformation, indicating that the existence of metal cobalt can improve wear resistance.

3.2. Abrasion

The abrasion wear rate as a function of the number of revolutions is plotted in Fig. 4. The wear rate of the two types of samples increases with the increasing load. The

(a)

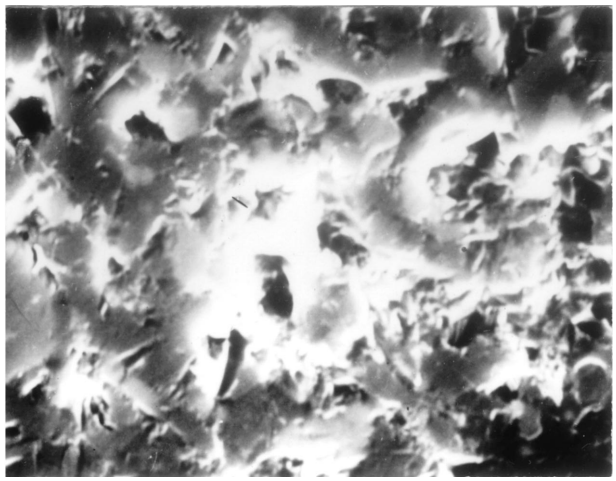

(b)

Figure 3 SEM images of the eroded surfaces of (a) AT_{30} and (b) ATC ceramics blasting velocity 90 m s^{-1}; impact angle, 90°; magnification ×5000.

result is quite similar with that obtained for many other ceramics [11], but there is no linear relation with load. It is shown that the abrasive wear loss increases with increasing hardness of the abradants. The hardness of sample is 1954 H_V. It is higher than that of SiO_2 (about 1350 H_V) and is lower than that of SiC (about 2500 H_V). The influence of particle hardness is obvious in the test. The wear loss caused by SiC abradants is far more than that caused by SiO_2 abradants. The effect of abradant hardness on wear resistance of the sample is consistent with work reported in the literature [12, 13].

Fig. 5 shows abrasion surface images of the test samples under 100 N with SiC particles after 4000 revolutions. Plastic deformation can be clearly seen in the abrasion surface of the ATC ceramic. Whereas intergranular cracks, pits and cluster spalling are shown in the surface of the AT_{30} ceramic.

The hardness and fracture toughness are very important mechanical properties that influence the abrasive wear resistance of brittle materials such as most ceramics [11]. Ceramics such as alumina can offer a high wear resistance due to their high hardness [14]. Compared with AT_{30} ceramic, the hardness of ATC ceramic is relatively low. It is indicated that the better resistance of ATC is probably due to its fracture toughness. Gahr

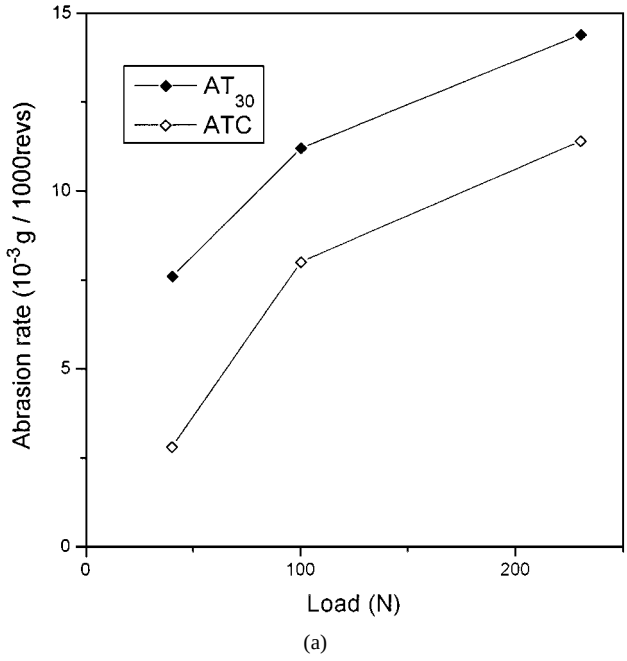

(a)

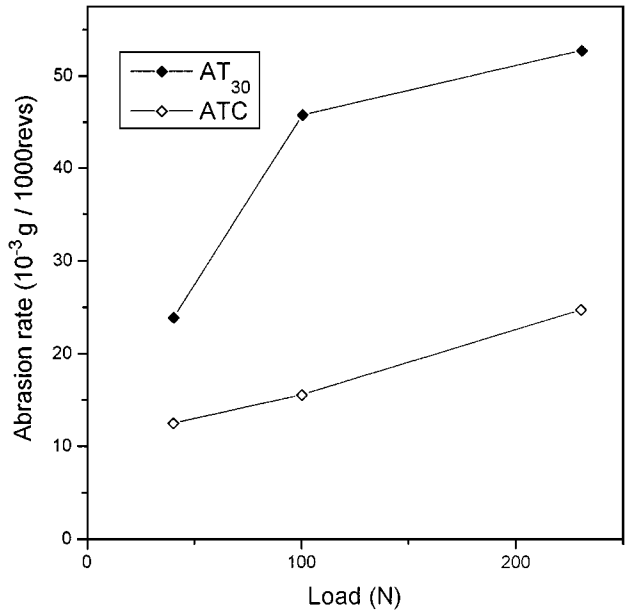

(b)

Figure 4 Abrasion wear rate of the test ceramics versus different load with (a) SiO_2 and (b) SiC particles.

also confirmed that when fracture toughness is lower than 10 MPa $m^{-1/2}$, wear resistance of the brittle materials mainly depends on fracture toughness. But from each figure the wear rate is somewhat different from that of $H_V^{1/2} \times K_{IC}^{-2}$ [15].

4. Discussion

The results show that the ATC ceramic possesses improved abrasion and erosion wear resistance. Its reasonable microstructure and mechanical properties caused by cobalt films existing at grain boundaries contribute to these. In abrasion wear, when the particles act on the ATC ceramic, the cobalt films can relax the stress concentration through plastic deformation. So cobalt increases the energy for crack nucleation and propagation along boundaries, which further enhances the

(a)

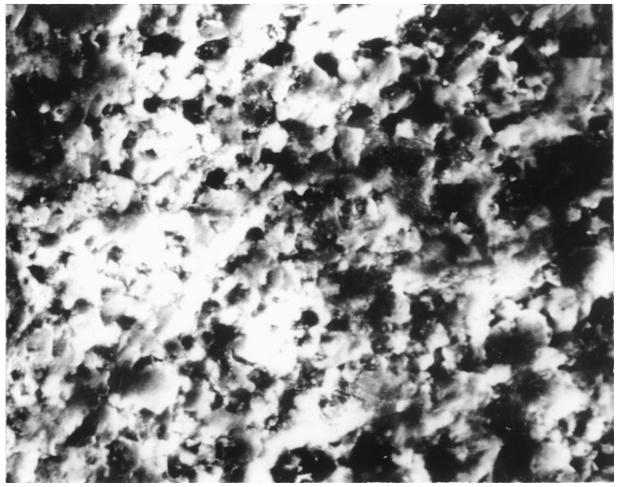

(b)

Figure 5 SEM images of abrasion wear surfaces of (a) AT_{30} and (b) ATC ceramics (magnification $\times 2000$).

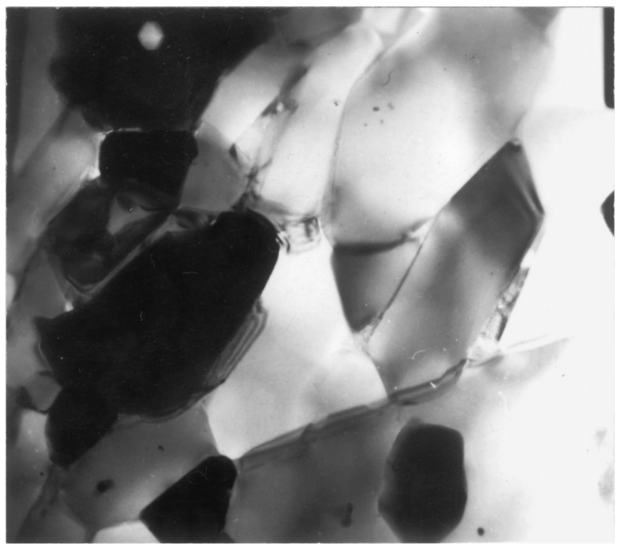

Figure 6 TEM polished surface image of ATC ceramic, showing thin cobalt films existing at the grain boundaries (magnification $\times 10\,000$).

mechanical properties and wear resistance of ATC ceramics.

Fig. 6 shows the TEM image of the ATC ceramic. The white grains are alumina, and the black grains are

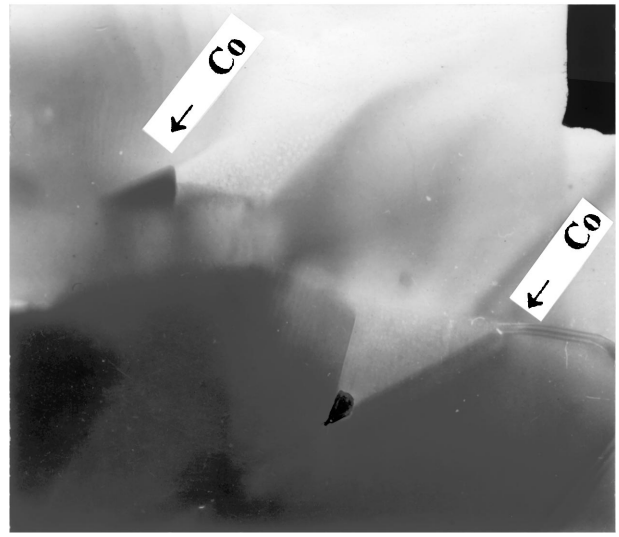

Figure 7 TEM polished surface image of ATC ceramic, showing metal cobalt can cover pores during sintering (magnification $\times 100\,000$).

TiC. Cobalt films located at the grain boundaries are clearly seen. The distribution of Al_2O_3 and TiC grains is homogeneous and the grains maintain their original angular shape, which is implied by the fact that the same kind of ceramic grains do not merge and grow during the sintering process. There are almost no pores in the matrix of the ATC ceramic. The cobalt films are very thin and form a three-dimensional net distributed on the interfaces. This structure can prevent or reduce reactions between Al_2O_3 and TiC. The most common reaction between Al_2O_3 and TiC is [1]

$$Al_2O_3 + TiC = Al_2O\uparrow + TiO + CO\uparrow$$

If the reactions occur at high temperature in the sintering process, a gas phase, and thus more pores, will consequently be produced in the sintered matrix. The strength of the ceramic will decrease with the increasing number of pores. Fig. 7 shows that cobalt is located at the grain boundaries, where the pores are often produced. The melting point of cobalt is much lower than the sintering temperature of 1600 °C. Cobalt is the fluid phase during sintering: it can fill the pores and cover the grains. Therefore, in contrast to AT_{30} ceramic, ATC has higher stiffness.

In the Al_2O_3–TiC ceramic system, the dispersion of TiC grains can prevent cracks from propagating, and therefore improve the properties of the Al_2O_3–TiC ceramics, especially the fracture toughness. For ATC ceramic, cobalt films coat the surface of Al_2O_3 and TiC powders to some extent, and thus the interface properties are changed. The bonding strength of the interface is supposedly increased, thus improving its mechanical properties. Besides intercrystalline fracture behaviour (see Fig. 8a), typical cleavage steps (including secondary cleavage steps) are clearly seen in Fig. 8b, which is caused by transcrystalline fracture. It is obvious that the development of bonding strength results in an increasing percentage of transcrystalline compared with intergranular fractures. This is because of the presence of cobalt in the grain boundaries, thus

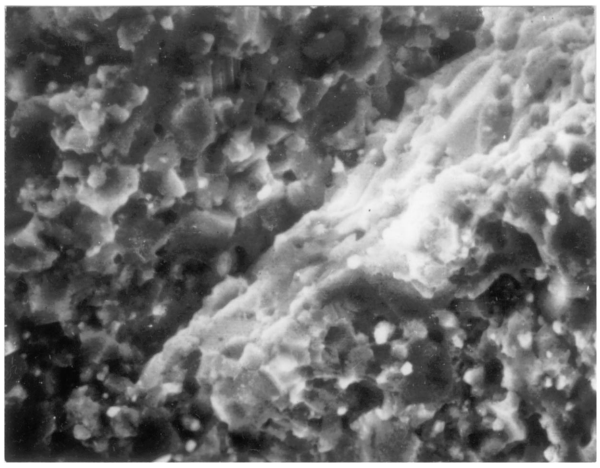

(a)

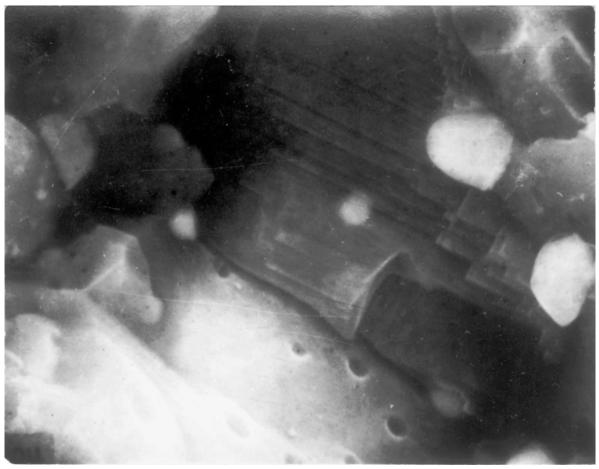

(b)

Figure 8 SEM images of the fracture surface of the ATC ceramic at $\times 2000$ (a) and $\times 10\,000$ (b) magnification.

the bonding strength between grains is increased, and is even higher than the fracture strength of some grains. Cobalt distributes along grain boundaries yielding an ATC ceramic with a relatively good ability to deform plastically, and does not easily result in cluster spalling.

At relatively higher impact angles, the impact kinetic energy of particles mainly turns into the propogation energy of cracks. High-angle erosion makes cracks in the AT_{30} ceramic propogate along grain boundaries. When those cracks connect with each other, grains are detached and thus cause the erosion of material. For the ATC ceramic, the crack propagation energy is raised through plastic deformation. With the same impact kinetic energy of SiC particles, the erosion resistance at high impact angles of ATC fine ceramic is mainly determined by its fracture toughness. At relatively lower erosion angles, besides the erosion mechanism mentioned above, there is also a plough erosion mechanism caused by hard abradants scratching on the surfaces of the test ceramics. The plough erosion rate decreases with increasing target hardness. The hardness of the AT_{30} ceramic is higher (20.98 H_V) and its ability to resist the cutting of SiC particles and plough erosion seems to be better than that of the ATC ceramic. But because of its much higher fracture toughness, it possesses a greater ability to resist fracture along boundaries. Summing up the two factors mentioned above, it can be concluded that the erosion rate at low impact angles of ATC fine ceramic is lower than that of AT_{30} ceramic.

Compared with AT_{30} ceramic, the abrasion wear surface of the ATC ceramic appears to be fine and smooth. Cobalt films form a three-dimensional net inside and a two-dimensional net on the surface of the sample, embedded with TiC and Al_2O_3 particles. When abradants scratch on the surface of the sample, cobalt appears to deform plastically and thus absorbs part of the energy acting on the particles. The plastic deformation is remarkable when some hard particles spall. On the other hand, it is displayed as cluster spalling. On the left of Fig. 5b there is a pellet spalling from the matrix. From its size and shape it can be estimated that it contains at least two particles. These granular pellets are formed by lateral cracks caused during the loading–unloading process of abradants on the surface. For "pure" brittle materials such as AT_{30} ceramic, once a lateral crack is formed, it developes quickly along weakly bonded grain boundaries. Cracks can cause cluster spalling more easily than in ATC ceramics.

5. Conclusions

The new process of preparing fine ATC ceramic made of Al_2O_3–TiC powders coated with a layer of cobalt film is an effective approach for improving the mechanical properties of brittle ceramic materials. The role of thin cobalt films coated on Al_2O_3 and TiC powders is important in the wear process. The bridging and anchoring effect of cobalt dispersion at grain boundaries is remarkable in toughening the matrix. In conclusion, the wear resistance of ATC ceramics is better than that of AT_{30} ceramics. Microcracking, single detachment and plastic deformation are the dominant mechanisms in wear damage of ATC ceramics. Crack propagation and cluster spalling are the main wear mechanisms of AT_{30} ceramics.

Acknowledgements

The research work is supported by the National Natural Science Foundation of China (NNSFC) under Contract No. 59 332 060. The authors thank engineer A. L. Zhang for experimental assistance.

References

1. M. LEE and M. P. BOROM, *Adv. Ceram. Mater.* **3** (1988) 38.
2. S. J. BURDEN, J. HONG, J. W. RUE and C. L. STROMBBORG, *Amer. Ceram. Soc. Bull.* **67** (1988) 1003.
3. S. F. WAYUE and S. T. BULJAN, *J. Amer. Ceram. Soc.* **72** (1989) 754.
4. R. P. WAHI and B. ILSCHNER, *J. Mater. Sci.* **15** (1980) 875.
5. S. Y. GUO, J. LI, D. S. MAO, M. H. XU and Z. Y. MAO, *Wear* **203–204** (1997) 319.
6. A. G. EVANS and T. R. WILSHAW, *Acta Metall.* **24** (1979) 939.

7. E. HORNBOGEN, *Wear* **33** (1975) 251.
8. M. A. MOORE and D. B. MARSHALL, *ibid*. **60** (1980) 123.
9. J. F. BELL and P. S. ROGERS, *Mater. Sci. Technol*. **3** (1987) 807.
10. A. G. EVANS, *J. Amer. Ceram. Soc*. **73** (1990) 187.
11. S. Y. GUO and Z. Y. MAO, in Proceedings of the Second Pacific Rim International Conference on Advanced Materials and Processing, 1995, pp. 2737–42.
12. R. C. D. RICHARDSON, *Wear* **11** (1968) 245.
13. S. V. PRASAD and P. D. CALVENT, *J. Mater. Sci*. **15** (1980) 1746.
14. K. H. ZUM GAHR, "Microstructure and Wear of Materials" (Elsevier, 1987) pp. 180–1.
15. *Idem*, *Met. Progr*. **116** (1979) 46.

Received 6 October 1997
and accepted 30 July 1998